International Journal of Energy Production and Management
Vol. 8, No. 2, June, 2023, pp. 71-79
Journal homepage: http://iieta.org/journals/ijepm

Enhancing Greenhouse Thermal Management with Flat Plate Solar Collectors and Al_2O_3-Water Nanofluid

Zhyan F. Hassan, Banipal N. Yaqob*, Ranj S. Abdullah

Department of Mechanical and Energy Engineering Techniques, Erbil Technical Engineering College, Erbil Polytechnic University, Erbil 44001, Iraq

Corresponding Author Email: banipal.yaqob@epu.edu.iq

https://doi.org/10.18280/ijepm.080203

Received: 27 November 2022
Accepted: 3 April 2023

Keywords:
flat plate solar collector, Al_2O_3-water nanofluid, collector efficiency, greenhouse heating, numerical simulation TRNSYS

ABSTRACT

Flat Plate Solar Collectors (FPSC) are one of the most environmentally friendly and energy-efficient heating solutions. In this work, the thermal performance of the FPSC for a greenhouse heating system was experimentally and numerically investigated by utilizing distilled water as a working fluid and Al_2O_3-water nanofluid with two different nanoparticle concentrations of 0.2wt.% and 0.5wt.%. The simulation model was conducted using TRNSYS 18, and its outcome was validated with experimental results. As a first step, the study estimates the maximum required amount of energy for a greenhouse in the Scientific Research Center at Erbil, Iraq. A temperature of 23℃ was selected as a set point temperature in the greenhouse, which is essential for the experiments needed for developing several plants. The most interesting finding was that when nanofluids were used as a working fluid, the efficiency gain was larger than with water only. The highest collector efficiency was attained when 0.5wt.% nanofluid was used in the FPSC, which increased the collector efficiency by 17.5% over the water case. Additionally, FR (UL) values for Al_2O_3-nanofluid and water are approximately close to each other, while for all applied concentrations, Al_2O_3-nanofluid's FR (τα) values were more significant than water. Further analysis showed that, during the coldest months of the year, the system could raise the inner air temperature of the greenhouse, which is ideal for farming applications.

1. INTRODUCTION

A greenhouse is a climate-controlled structure that shields plants from adverse climatic conditions [1]. Because the need for agricultural resources is expanding, greenhouse agriculture is a growing sector in several countries. Consequently, greenhouse food production provides an alternative method for meeting year-round food demand increases. The first concern for the greenhouse is to install a suitable heating system during cold weather that can maintain a comfortable temperature while it can conserve energy outside of the cultivation season. Therefore, it is crucial to provide a low-cost heating system to ensure optimal indoor temperatures throughout the cold months. Various renewable energy sources, including solar, geothermal, and biomass energy, could be utilized for a greenhouse heating system instead of fossil fuels; also solar thermal energy systems have been studied [2-4].

Evacuated tube, flat plate, and unglazed plastic collectors are the most prevalent types of SWHS. Flat plate solar collectors are inexpensive stationary collectors that are easy to fabricate and simple to install. Moreover, they require lower cost of operation and maintenance as compared to other solar collector types. A greenhouse can reduce the demand for fossil fuels for heating and help overcome climate variability with solar energy. Esen and Yuksel [5] experimentally investigated three different heating methods for greenhouse heating, (i) a solar system, (ii) biogas, and (iii) ground energy. The results demonstrated that renewable energy could be employed for greenhouse heating and the systems achieved their functions. Attar et al. [6] assessed and investigated the greenhouse heating efficiency of a solar water system using a TRNSYS simulation. They demonstrated that a flat plate collector might raise the indoor air temperature in a greenhouse by 5℃.

Generally, the most effective solar heaters are the flat plate solar collectors. Nevertheless, these collectors have low thermal efficiency and outlet temperatures [7, 8]. Since then, several techniques have been offered to improve their efficiency and thermal performance [9-11]. The working fluid is one of the most essential aspects that affects the performance of flat plate solar collectors [12]. Many studies have been carried out to enhance the performance of the collector, by rising the thermal behaviour of the collector's working fluid through utilizing nanofluids [13-16]. Dispersing nanoparticles in the base fluid directly affects the thermophysical properties of the nanofluid, such as thermal conductivity, viscosity, density and specific heat [8], and numerous studies have previously investigated these physical properties [17-19]. The main aim of using nanofluids is to reach the maximum allowable thermal conductivity at the minimum possible concentration of nanoparticles; this is the primary property of nanofluids [20]. However, the pressure drops and the primary disadvantages of using nanofluids are the stability of the nanoparticles in the base fluid [21]. Numerical investigations have been performed by Genc et al. [13] to find the effect of Al_2O_3-water nanofluid on the

efficiency of a FPSC with different volume fraction and mass flow rate. Their results indicate that using nanofluid as working fluid increases efficiency in comparison with water. Using CeO_2-H_2O nanofluid to enhance the efficiency of flat plate solar collector was experimentally examined by Sharafeldin and Gróf [22]. They found that employing this nanofluid improves collector efficiency by 10.74% to water zero value of reduced temperature parameter $(T_i - T_a)/G_T$. The performance of flat plate solar collector employing Al_2O_3/DDW nanofluid with different volume fractions ranging from 0.1% to 3% was theoretically and experimentally studied by Hawwash et al. [23]. Their results reveal that utilizing alumina nanofluid enhances collector thermal efficiency by around 3% and 18% compared to water. Also, same thermal performance enhancement was found by Tong et al. [24] when they utilizing various working fluids in an experimental setting (water, Al_2O_3, and CuO). The results of their study showed that using different nanofluids in the flat plate solar collector could improve thermal efficiency compared to the water case and that using 1vol% Al_2O_3 gives the best performance to the flat plate solar collector. Furthermore, more researchers [25-28] investigated the effect of adding nanofluid into the flat plate solar collectors using different mass flow rates and different nanoparticles. All results indicated an improvement in the thermal efficiency of the FPSCs.

Much reported research has been carried out on FPSC for greenhouse heating systems. However, no research has been done on utilizing nanofluid as a working fluid for that purpose yet. This study's foremost objective is to investigate experimentally and numerically the opportunity of using SWHS for a greenhouse heating system using Al_2O_3-water nanofluid as a working fluid for Kurdistan Region-Iraq and to encourage the ministry of agriculture and farmers to adopt this system. Solar heating greenhouses might be an option in Kurdistan because of the region's sunny climate, which means decreasing heating costs and less gas pollution. Furthermore, the analysis is carried out using the TRNSYS modelling program according to Erbil weather.

2. MATHEMATICAL ANALYSIS

2.1 Heat load calculation

The maximum greenhouse heating load required is calculated based on the minimum ambient air temperature, which occurs in the coldest day of the year. The greenhouse overall thermal losses are calculated as follows [29]:

$$Q_{Gloss} = U\, A_G (T_r - T_a) \tag{1}$$

where, A_G is the greenhouse surface area, T_r the room design temperature and T_a the ambient temperature.

The quantity of heat lost from a greenhouse depends on the structure heat loss. Conduction, convection, and radiation are the most common heat transfers from a greenhouse. In a heat loss equation, all three losses are usually added together as a coefficient to figure out how much heat a greenhouse needs, and *U* refers to the energy loss coefficient, that can be given by the study of [30]:

$$U = \frac{1}{R_{total}} \tag{2}$$

where, R_{total} is the total thermal resistance of the materials, calculated from the following equation:

$$R_{total} = \frac{1}{h_i} + \frac{x}{k_m} + \frac{1}{h_o} \tag{3}$$

where, h_i and h_o are interior and exterior wall surface convective heat transfer coefficient, respectively, x shows the thickness of the material, and k_m is the material thermal conductivity.

The heat supply from the storage tank to the greenhouse depends on the amount of greenhouse heat required, which varies with the time. The following expression gives the heat transfer rate, Q_{Hu} supplied by the heat exchanger to the greenhouse [29]:

$$Q_{Hu} = \dot{m}_H C_p (T_{Hi} - T_{Ho}) \tag{4}$$

where, $\dot{m}_H$ is the total mass flow rate through the heat exchanger, C_p the heat capacity of working fluid, T_{Ho} and T_{Hi} are the temperatures of the water exiting and entering the heat exchanger, respectively.

To calculate the thermal performance of FPSCs, first the useful heat gain (Q_{Cu}) from FPSC's needs to be calculated as follows [31]:

$$Q_{Cu} = \dot{m}_C C_p (T_{Co} - T_{Ci}) \tag{5}$$

where, $\dot{m}_C$ is the collector fluid mass flow rate, T_{Co} and T_{Ci} are collector exiting and entering fluid temperatures.

On the other hand, to show the effect of the collector optical properties and heat losses, the usable energy gained by the working fluid can also be represented as given below:

$$Q_u = F_R A_c [G_T(\tau\alpha) - U_L(T_{Ci} - T_a)] \tag{6}$$

where, F_R is the collector heat removal factor, A_c the gross area of the collector, G_T the intensity of solar radiation, $\tau\alpha$ the effective absorptance–transmittance product, U_L the overall heat transfer coefficient, T_{Ci} the input fluid temperature and T_a the ambient temperature.

The flat plate solar collector thermal efficiency η_{th} can be estimated by:

$$\eta_{th} = \frac{Q_{Cu}}{G_T A_c} \tag{7}$$

Additionally, the thermal efficiency can be given as follows:

$$\eta_{th} = F_R(\tau\alpha) - F_R(U_L)\left(\frac{T_{Ci} - T_a}{G_T}\right) \tag{8}$$

The instantaneous efficiency is determined from Eq. (7) and is planned as a result of reduced temperature parameter $(T_{Ci} - T_a)/G_T$. Based on the Eq. (8), assuming U_L, F_R, and $(\tau\alpha)$ all remained the same, the plots of η_{th}, versus $(T_{Ci} - T_a)/G_T$ would be straight lines with intercept $F_R(\tau\alpha)$ and slope $(-F_R U_L)$.

Dispersing nanoparticles into the base fluid strongly impacts the thermophysical properties of nanofluids [32]. Water and Al_2O_3-nanoparticles thermophysical properties are presented in Table 1. The mixture's thermal conductivity (k) can be calculated using the following formula [33]:

$$k_{nf} = k_{bf}\left[\frac{k_p + 2k_{bf} - 2\varphi(k_{bf} - k_p)}{k_p + 2k_{bf} + \varphi(k_{bf} - k_p)}\right] \quad (9)$$

The nanofluid density (ρ) is determined by applying the following equation [34]:

$$\rho_{nf} = (1-\varphi)\rho_{bf} + \varphi\rho_{np} \quad (10)$$

While the nanofluid's heat capacity (C_p) is calculated as follows [35]:

$$C_{p,nf} = \frac{(C_p\rho)_{bf}(1-\varphi) + (C_p\rho)_{np}(\varphi)}{\rho_{nf}} \quad (11)$$

Additionally, the viscosity (μ) of the nanofluid is found as follows [36]:

$$\mu_{nf} = \mu_{bf}(1 + 2.5\varphi) \quad (12)$$

where, φ is particle concentration by weight (%), bf specifies the base fluid, np indicates the nanoparticle, and nf shows the nanofluid.

Table 1. Thermophysical properties of the working fluids

Particle & base fluid	Particle size (nm)	k (W/m·K)	C_p (J/kg·K)	ρ (kg/m^3)	μ (mPa.s)
Water	-	0.605	4179	997.1	0.89
Al_2O_3	50	40	773	3960	-
Al_2O_3-Water (0.2wt.%)	-	0.6085	4152.1	1003.0	0.895
Al_2O_3-Water (0.5wt.%)	-	0.6137	4112.4	1011.9	0.901

3. NANOFLUID MATERIALS AND PREPARATION

3.1 Preparation method of the nanofluid

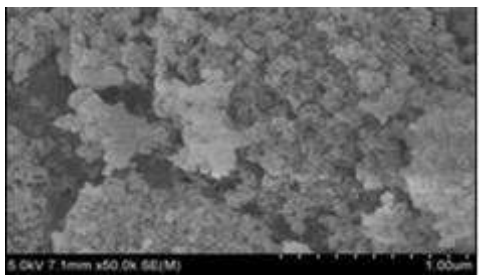

Figure 1. SEM image of Al_2O_3 nanoparticles

The working fluid used in this study is distilled water (DW) as a first run and water-based Al_2O_3 nanoparticle white powders with a purity of 99.9+% as a second run; SEM images of nanoparticles are shown in Figure 1. The Al_2O_3 nanoparticles are simple to make, inexpensive compared to other metal oxide nanoparticles [37], and have excellent thermal conductivity. A technique has been used to minimize Al_2O_3 agglomeration and rising dispersion behaviour by dispersing Al_2O_3 powder nanoparticles in distilled water as the base fluid. First, the nanoparticles were added to distilled water and dissolved by a magnetic stirrer for 10 minutes. Secondly, an ultrasonic homogenizer (40 kHz frequency) was utilized for approximately 15 minutes to disseminate the nanoparticle mixture and decrease agglomeration, as shown in Figure 2.

Figure 2. Magnetic stirrer and ultrasonic homogenizer

3.2 Experimental setup and procedures

The experimental prototype was set up in the Scientific Research Center in Erbil city (36.2 N latitude and 44 E longitude). A schematic view of the system setup is explained in Figure 3. The system consists of ten flat plate solar collector panels set in two parallel rows (five by five) tilted southward at 60º, as shown in Figure 4 with technical specifications given in Table 2, pumps (SPERONI, SCR 25/80-180), a storage tank with 1000 liters in capacity and with two immersed straight-tube heat exchangers, pipe, residential water softener and measurement equipment like temperature sensors (type QAP21.2 and QAE26.9 with measuring accuracy of ±1.65 K in the range (-30 to +180)°C and ±1.75 K in the range (-50 to +180)°C, respectively), pressure transducers (with pressure range of 0-10 bar with 0.4% accuracy of full scale), flow meters (measuring range of 1-1.92 m^3/h). In the first test, distilled water was used to transfer heat from the solar collectors to the storage tank. The working fluid was circulated through the system using circulating pumps. In the second test, nanofluid was used in the closed-loop connecting the solar collectors with the storage tank instead of distilled water.

Table 2. Technical specification of the FPSCs

Content	Description
Collector gross surface	2.353 m²
Absorber surface	2.138 m²
Weight	44 kg
Length x width x depth	2150×1090×100 mm
Cover	3.2 mm protection glass, super transparent, hailstone secure
Absorber material	Copper on copper plate
Insulation rear wall	40 mm mineral wool 70 kg/m^3 with fiberglass
Insulation side wall	30 mm mineral wool

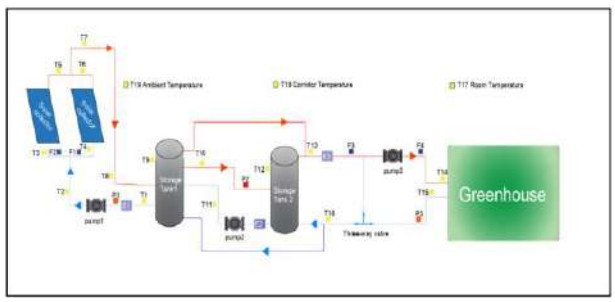

Figure 3. Experimental setup of SWHS

Figure 4. Photograph of the FPSC

A greenhouse with 85.8 m^3 in volume was installed in the backyard of the building with a horizontal buried heat exchanger type (PE-XC EVOH) with 1-inch in diameter placed at 10 cm underground, as shown in Figure 5.

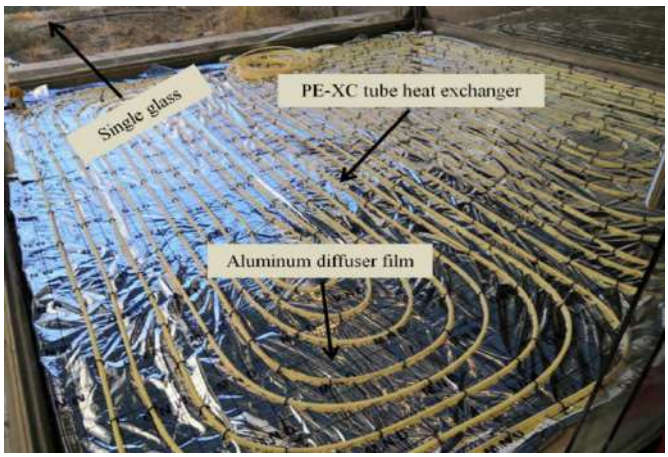

Figure 5. The type (PE-XC EVOH) heat exchanger buried in the greenhouse

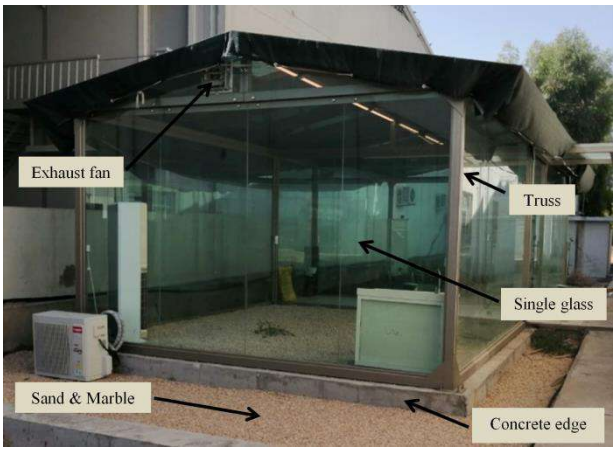

Figure 6. Schematic of the test greenhouse external view

The walls and the roof were made of a single glass of 1 cm thickness, as shown in Figure 6. The heat stored in the tank is pumped through the buried heat exchanger, where it heats the greenhouse space to get the setting temperature (23℃ in this case).

Each measuring signal has been transferred to a computer monitor using DESIGO INSIGHT program. Pyrometer type (LP02) was used to measure the solar radiation over the complete solar spectrum range of 285 to 3000 nm and maximum irradiance of 2000 W/m^2. Measured data were recorded and stored using a read-out device/data-logger (LI19).

4. UNCERTAINTY ANALYSIS

The precision of the results obtained is determined by uncertainty analysis. Because of the inaccuracies generated by data reading, instrument selection, test circumstances, surroundings, observance, and other factors, uncertainty analysis should be performed regardless of how appropriate the instruments are. The primary causes of uncertainty in collector efficiency estimation include errors in solar irradiance, mass flow rate, and temperature measurements. The standard deviation and mean of different measurements are included in the Gaussian distribution approach and are given as in Eq. (13) [38]:

$$U_x = \pm\left(2\frac{\sigma_n}{x_n}\right) \times 100 \tag{13}$$

where, U_x represents measurement uncertainty, σ signifies the measured data's standard deviation, and x_n symbolizes the measured parameter's mean. The suffix n indicates the number of measurements. The uncertainties of the primary apparatuses utilized in this investigation are shown in Table 3.

Table 3. The uncertainty of the measuring devices

Measuring device	Uncertainty (%)
Pyranometer	±1.08
Flow meter	±0.85
Thermometer	±2.3

5. NUMERICAL SIMULATION MODEL

The SWHS model explored in this study was developed using TRNSYS 18. The schematic layout of the SWHS model using the TRNSYS program is shown in Figure 7.

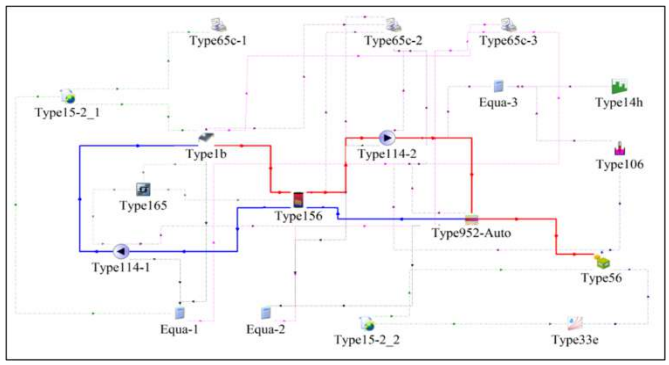

Figure 7. TRNSYS modelling of the SWHS

6. RESULTS AND DISCUSSIONS

The experimental, in sunny days, and TRNSYS simulation programs were utilized to investigate the collector's performance for greenhouse heating. These investigations were carried out over several days. Moreover, the data were collected every 15 minutes from 8:00 to 16:00. The collector's efficiency was evaluated in terms of working fluid concentration (water, Al_2O_3-nanofluid) under an extensive range of operating conditions.

6.1 TRNSYS model validation

The system was first tested using water as a working fluid, and then the water was replaced with Al_2O_3-water nanofluid. The experimental work and TRNSYS simulation program provide information on the fluctuations of the FPSCs inlet and outlet temperatures and the temperature differences as in Figure 8 for water and in Figure 9 for Al_2O_3-water. The maximum percentage error between experimental and simulation results were 7.9% and 6.4% for inlet and outlet collector water temperature, respectively, while for Al_2O_3-water nanofluid were 6.8% and 4.5%, respectively. Additionally, the solar irradiance experimental, measured data and predicted data using TRNSYS simulation program are presented in Figure 10 with approximately 10% maximum error.

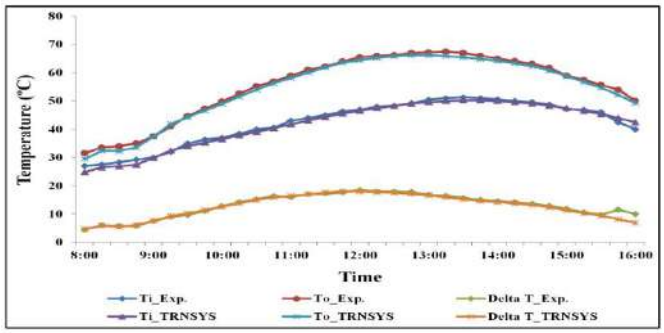

Figure 8. Comparison between the simulation and experimental results for FPSC water temperature

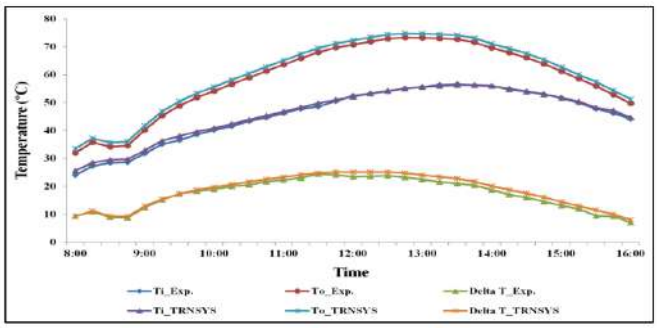

Figure 9. Comparison between experimental and simulation temperatures of the collectors' nanofluid for 0.2wt.% concentration

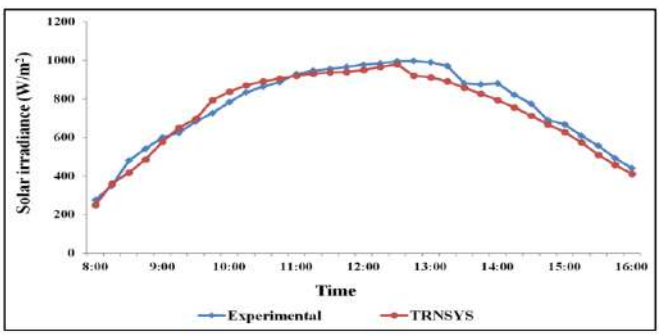

Figure 10. Solar irradiance verification comparing experimental and simulation results

The verification results show a good agreement between experimental and simulation results that closely match with acceptable accuracy. From the figures above, it can be concluded that the TRNSYS simulation program is a useful tool that can be adopted for simulating the present solar water heating system.

6.2 Comparisons between the working fluids

The variation of collector outlet temperature with time is illustrated in Figure 11 for two different working fluids, water and nanofluid (0.2wt.% and 0.5wt.%) and a constant mass flow rate of 0.2 kg/s.

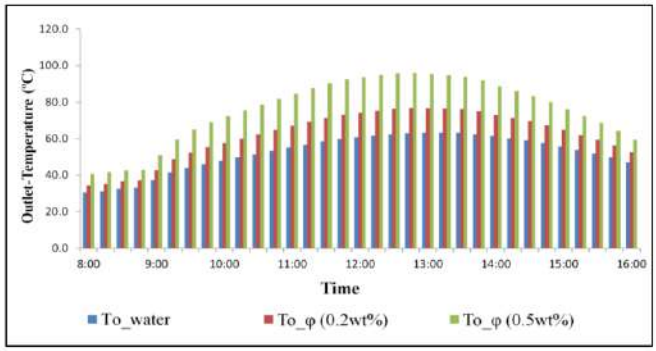

Figure 11. Collectors' outlet temperature at different working fluids

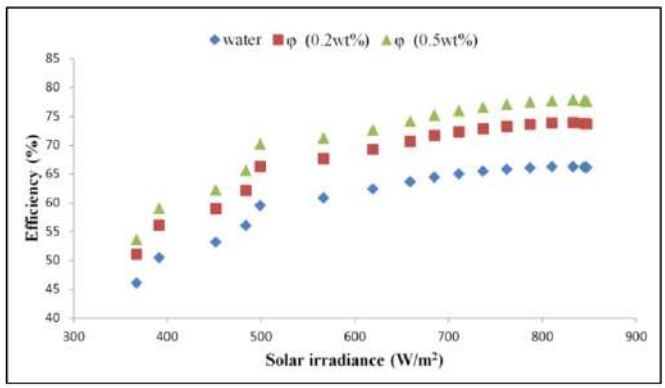

Figure 12. Efficiency versus solar irradiance for DW and for nanofluid with different concentration

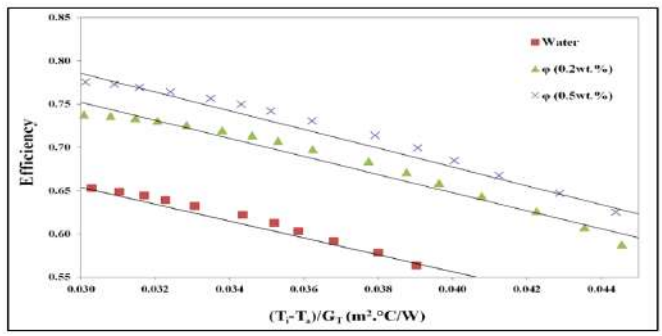

Figure 13. FPSC efficiency for DW and for Al_2O_3-water nanofluid with two different concentrations

Figure 11 indicates that the results for Al_2O_3-water nanofluid are higher than those using water. This is expected since Brownian motion increases the nanoparticle's conduction and convection heat transfer [39]. Moreover, by comparing the collector outlet temperature of nanofluids with

two different concentrations, it can be noticed that the outlet temperature of 0.5wt.% is higher than that of 0.2wt.%, which were 96.1°C and 76.8°C, respectively. Consequently, it can be concluded that adding nanoparticles to a base fluid increases the effect of temperature increase.

Figure 12 shows the variation of the FPSC efficiency with solar irradiance for two working fluids (i) DW, and (ii) Al_2O_3-water nanofluids, with two nanoparticle concentrations of 0.2wt.% and 0.5wt.%. It can be noticed that as the solar irradiation increases, the collector performance goes up. However, it is worth noting that the collector's thermal efficiency in the case of using Al_2O_3-water nanofluids at a concentration of 0.5wt.% is about 80% which is higher than in the other two cases.

However, Figure 13 depicts the efficiency of solar collectors as a function of reduced temperature parameter $(T_{Ci} - T_a)/G_T$ for DW and for Al_2O_3-water nanofluid with different concentration. The maximum collector efficiency was 66.3%, 74% and 78% for DW, and Al_2O_3-water nanofluid (0.2wt.% and 0.5wt.%), respectively. Optimum efficiency was reached when nanofluid with 0.5wt.% concentration was utilized, which improved the collectors' efficiency by 17.5 % compared to the water case.

Moreover, the absorbed energy parameter $F_R(\tau\alpha)$ and removed energy parameter $F_R(U_L)$ for FPSC are listed in Table 4 when water and Al_2O_3-water nanofluid were used. The results show that the $F_R(\tau\alpha)$ for water values is 0.654 and for Al_2O_3-water nanofluid 0.752 and 0.785 for 0.2wt.% and 0.5wt.% concentration, respectively. $F_R(U_L)$ values for Al_2O_3-nanofluid and water are close to each other since the slopes of models are negative. It can be observed that the $F_R(\tau\alpha)$ values of nanofluid are higher than those obtained utilizing water for all involved concentrations. Moreover, when a concentration of 0.5wt.% was used, the highest value was achieved, higher by 20% compared to the water case.

The pump enhanced the collisions between liquid molecules and solid particles by increasing the random motion of the particles. The thermal conductivity of the nanofluid is greater than that of DW, and this is because of the Brownian motion, which plays an essential factor in this improvement. It is also worth noting that turbulent fluid flow has been attained. This is caused by the convective heat transfer coefficient and the efficiency of the FPSC by using nanofluid being greater than using water.

Table 4. Values of FR (τα)and FR (UL)for different working fluids

Base fluid type	$F_R(\tau\alpha)$	$F_R(U_L)$ W/m².°C	R^2
Water	0.654	-9.7765	0.9614
0.2wt.% Al_2O_3-nanofluid	0.752	-10.429	0.9642
0.5wt.% Al_2O_3-nanofluid	0.785	-10.822	0.9672

6.3 Greenhouse heating load

The greenhouse heating load is calculated using Eq. (1). The maximum estimated value was 12.8 kW, which was obtained during the coldest day of the winter season, (12th January 2022 at 6:00 A.M), when the minimum ambient air temperature recorded was 0°C. Therefore, as illustrated in Figure 14, the primary heat loss from the greenhouse happens during the night hours.

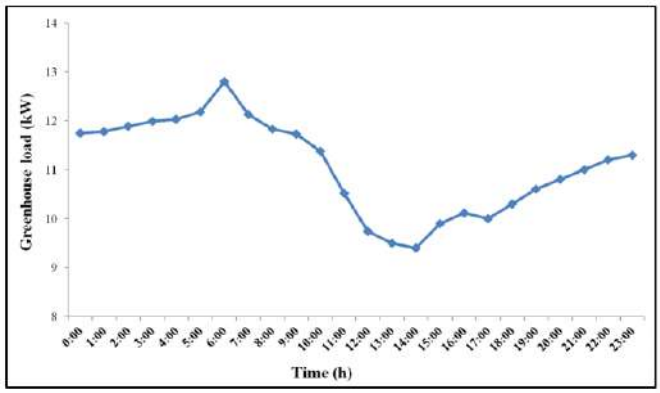

Figure 14. Greenhouse heating load value on 12th January

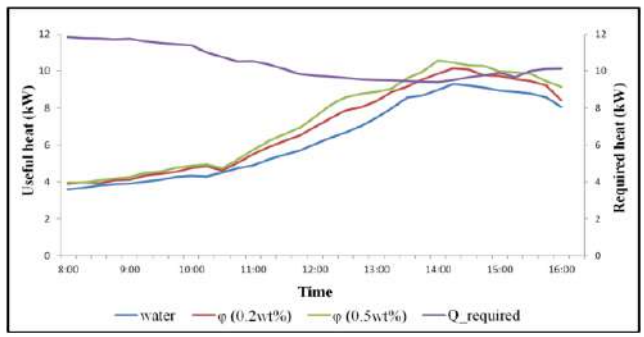

(a)

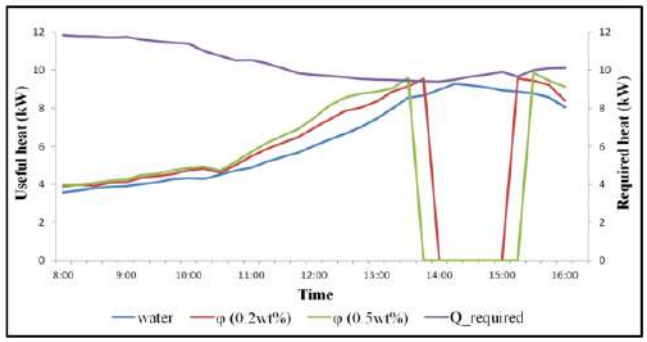

(b)

Figure 15. Greenhouse heating load vs. energy provided (heat supply). (a) non set-point temperature; (b) with set-point temperature

Energy is provided to the greenhouse if the inside air temperature obtained from the dynamic model is less than the design temperature set at 23ºC. Figures 15(a) and (b) show that the greenhouse supplied useful heat for winter's coldest day (12th January) without set temperature and set point temperature, respectively. The results show the heat supply to the greenhouse with different working fluids of DW and Al_2O_3-water nanofluid. As shown in these figures, the required heating load of the greenhouse has the highest value of 11.83 kW at the beginning of the day. In contrast, the supply heat from the collectors and the useful heat from the storage tank have the lowest value in the morning due to the sun's position and the highest value after solar noon, as illustrated in Figure 15(a). The maximum useful heat from the system continuously without any setting temperature was 9.29 kW, 10.14 kW, and 10.55 kW for water, and nanofluid (0.2wt.% and 0.5wt.%), respectively.

Figure 15(b) indicates that when the greenhouse

temperature reaches the set point temperature, the system is automatically turned off until the greenhouse temperature gets down to the set point temperature. The results show that the required temperature of the greenhouse could not be reached when water was used as the working fluid for this typical day. Further analysis showed that the system produces more useful heat when different nanofluid concentrations than water is used and the set point temperature was reached in the greenhouse. On the other hand, it is worth noting that the solar system may produce more heat for heating the greenhouse as ambient temperatures rise, which would reduce greenhouse heating demand.

Table 5 illustrates greenhouse average useful heat during January, February, and March. The maximum heat supply to the greenhouse was during March (2643.9, 3168.7, and 3212.2) kWh for DW and 0.2wt.% and 0.5wt.% Al_2O_3-water nanofluid, respectively.

Table 5. Average monthly greenhouse useful heat in (kWh)

Month	Water	Al_2O_3-water nanofluid (0.2wt.%)	Al_2O_3-water nanofluid (0.5wt.%)
January	2288.13	2793.99	2889.60
February	2451.37	2913.26	3003.53
March	2643.92	3168.71	3212.20

7. ECONOMIC ANALYSIS

In this section, the SWHS cost, energy cost, and payback time are compared with the price of a water heating system with electricity by conducting an economic analysis of the water heaters. The payback period refers to the time it takes for an investment to earn back its initial cost or the time it takes for an investor to break even. The SWHS used in this investigation costs a total of $50,400; in Erbil city, the cost of one kWh of electricity is $0.23 according to the Ministry of Electricity in Kurdistan region [40]. The SWHS costs and payback period are reported in Table 6. Interestingly, the data in this table show that the system payback duration is about 6 years when using nanofluid as a working fluid, while when using water, it is about 7 years.

Table 6. The costs and payback period of the SWHS

	Water	Nanofluid
Gain of energy (kWh/year)	30685.56	37506.25
Annual payment saving ($/year)	7057.68	8626.44
Payback of SWHS (year)	7.14	5.84

8. CONCLUSION

The impacts of various nanoparticle concentrations of Al_2O_3-water nanofluid as a working fluid in an FPC have been investigated experimentally and numerically. The SWH was installed to create a suitable condition in a greenhouse during the cold season. Two different concentrations, 0.2wt.% and 0.5wt.%, were tested at a fixed mass flow rate 0.2 kg/s. The following conclusion can be drawn:

1. Using Al_2O_3-water nanofluid produces better outcomes and increases collector efficiency compared to the DW, even with a low concentration of nanoparticles. Using 0.5wt.% of nanofluid increases the collector efficiency by 17.5% over the water case.
2. The absorbed energy parameter $F_R(\tau\alpha)$ values of Al_2O_3-water nanofluid for all concentrations are higher than using water. When a nanoparticle concentration of 0.5wt.% is used, there is a 20% increase in this factor compared to using water.
3. The maximum estimated value of the greenhouse heating load is 12.8 kW. The maximum heat supply to the greenhouse is during March (2643.9, 3168.7, and 3212.2) kWh for DW and 0.2wt.% and 0.5wt.% Al_2O_3-water nanofluid, respectively.
4. The greenhouses are big energy consumers. However, using nanofluids as HTFs, the system can produce and store more energy and then raise the inside temperature during the night and thus, reduce the waste of external energy sources.
5. The greenhouses have significant economic potential in the agriculture sector of Kurdistan. The economic feasibility analysis concluded that greenhouse SWHS with an FPSC is a cost-effective and profitable heating system. Using nanofluid instead of water as a working fluid yields significant economic results, where the system payback period is about 6 years compared to water, which is about 7 years.

ACKNOWLEDGMENT

It is a pleasure to appreciate the General Director of Scientific Research Center at Erbil Polytechnic University Asst. Prof. Dr. Hayman Kakakhan Awla and his colleagues for their technical supports and help. Also, all authors express their appreciation to Asst. Prof. Dr. Nazar Faraj Antwan for his valuable scientific advice.

REFERENCES

[1] Joudi, K.A., Hasan, M.M. (2013). Cooling and heating a greenhouse in Baghdad by a solar assisted desiccant system. Journal of Engineering, 19(8): 933-951.

[2] Chau, J., Sowlati, T., Sokhansanj, S., Preto, F., Melin, S., Bi, X. (2009). Economic sensitivity of wood biomass utilization for greenhouse heating application. Applied Energy, 86(5): 616-621. https://doi.org/10.1016/j.apenergy.2008.11.005

[3] Cuce, E., Harjunowibowo, D., Cuce, P.M. (2016). Renewable and sustainable energy saving strategies for greenhouse systems: A comprehensive review. Renewable and Sustainable Energy Reviews, 64: 34-59. https://doi.org/10.1016/j.rser.2016.05.077

[4] Taki, M., Rohani, A., Rahmati-Joneidabad, M. (2018). Solar thermal simulation and applications in greenhouse. Information Processing in Agriculture, 5(1): 83-113. https://doi.org/10.1016/j.inpa.2017.10.003

[5] Esen, M., Yuksel, T. (2013). Experimental evaluation of using various renewable energy sources for heating a greenhouse. Energy and Buildings, 65: 340-351. https://doi.org/10.1016/j.enbuild.2013.06.018

[6] Attar, I., Naili, N., Khalifa, N., Hazami, M., Farhat, A. (2013). Parametric and numerical study of a solar system for heating a greenhouse equipped with a buried

exchanger. Energy Conversion and Management, 70: 163-173. https://doi.org/10.1016/j.enconman.2013.02.017

[7] Hawwash, A.A., Ahamed, M., Nada, S.A., Radwan, A., Abdel-Rahman, A.K. (2021). Thermal analysis of flat plate solar collector using different nanofluids and nanoparticles percentages. IEEE Access, 9: 52053-52066. https://doi.org/10.1109/ACCESS.2021.3060004

[8] Zayed, M.E., Zhao, J., Du, Y., Kabeel, A.E., Shalaby, S.M. (2019). Factors affecting the thermal performance of the flat plate solar collector using nanofluids: A review. Solar Energy, 182: 382-396. https://doi.org/10.1016/j.solener.2019.02.054

[9] Pandya, H., Behura, A.K. (2017). Experimental study of V-through solar water heater for tilt angle and glass transmissivity. Energy Procedia, 109: 377-384. https://doi.org/10.1016/j.egypro.2017.03.034

[10] Zhu, Y., Shi, J., Huang, Q., Fang, Y., Wang, L., Xu, G. (2017). A superhydrophobic solar selective absorber used in a flat plate solar collector. RSC advances, 7(54): 34125-34130. https://doi.org/10.1039/C7RA04238H

[11] Bhowmik, H., Amin, R. (2017). Efficiency improvement of flat plate solar collector using reflector. Energy Reports, 3: 119-123. https://doi.org/10.1016/j.egyr.2017.08.002

[12] Kiliç, F., Menlik, T., Sözen, A. (2018). Effect of titanium dioxide/water nanofluid use on thermal performance of the flat plate solar collector. Solar Energy, 164: 101-108. https://doi.org/10.1016/j.solener.2018.02.002

[13] Genc, A.M., Ezan, M.A., Turgut, A. (2018). Thermal performance of a nanofluid-based flat plate solar collector: A transient numerical study. Applied Thermal Engineering, 130: 395-407. https://doi.org/10.1016/j.applthermaleng.2017.10.166

[14] He, Q., Zeng, S., Wang, S. (2015). Experimental investigation on the efficiency of flat-plate solar collectors with nanofluids. Applied Thermal Engineering, 88: 165-171. https://doi.org/10.1016/j.applthermaleng.2014.09.053

[15] Michael Joseph Stalin, P., Arjunan, T.V., Matheswaran, M.M., Dolli, H., Sadanandam, N.J.J.O.T.A. (2020). Energy, economic and environmental investigation of a flat plate solar collector with CeO_2/water nanofluid. Journal of Thermal Analysis and Calorimetry, 139: 3219-3233. https://doi.org/10.1007/s10973-019-08670-2

[16] Yousefi, T., Veysi, F., Shojaeizadeh, E., Zinadini, S. (2012). An experimental investigation on the effect of Al_2O_3–H_2O nanofluid on the efficiency of flat-plate solar collectors. Renewable Energy, 39(1): 293-298. https://doi.org/10.1016/j.renene.2011.08.056

[17] Sang, L., Liu, T. (2017). The enhanced specific heat capacity of ternary carbonates nanofluids with different nanoparticles. Solar Energy Materials and Solar Cells, 169: 297-303. https://doi.org/10.1016/j.solmat.2017.05.032

[18] Dalkılıç, A.S., Yalçın, G., Küçükyıldırım, B.O., Öztuna, S., Eker, A.A., Jumpholkul, C., Nakkaew, S., Wongwises, S. (2018). Experimental study on the thermal conductivity of water-based CNT-SiO_2 hybrid nanofluids. International Communications in Heat and Mass Transfer, 99: 18-25. https://doi.org/10.1016/j.icheatmasstransfer.2018.10.002

[19] Dalkılıç, A.S., Açıkgöz, Ö., Küçükyıldırım, B.O., Eker, A.A., Lüleci, B., Jumpholkul, C., Wongwises, S. (2018). Experimental investigation on the viscosity characteristics of water based SiO_2-graphite hybrid nanofluids. International Communications in Heat and Mass Transfer, 97: 30-38. https://doi.org/10.1016/j.icheatmasstransfer.2018.07.007

[20] Ganvir, R.B., Walke, P.V., Kriplani, V.M. (2017). Heat transfer characteristics in nanofluid—A review. Renewable and sustainable energy reviews, 75: 451-460. https://doi.org/10.1016/j.rser.2016.11.010

[21] Yu, W., Xie, H. (2012). A review on nanofluids: preparation, stability mechanisms, and applications. Journal of Nanomaterials, 2012: 1-17. https://doi.org/10.1155/2012/435873

[22] Sharafeldin, M.A., Gróf, G. (2018). Experimental investigation of flat plate solar collector using CeO_2-water nanofluid. Energy Conversion and Management, 155: 32-41. https://doi.org/10.1016/j.enconman.2017.10.070

[23] Hawwash, A.A., Rahman, A.K.A., Nada, S.A., Ookawara, S. (2018). Numerical investigation and experimental verification of performance enhancement of flat plate solar collector using nanofluids. Applied Thermal Engineering, 130: 363-374. https://doi.org/10.1016/j.applthermaleng.2017.11.027

[24] Tong, Y., Lee, H., Kang, W., Cho, H. (2019). Energy and exergy comparison of a flat-plate solar collector using water, Al_2O_3 nanofluid, and CuO nanofluid. Applied Thermal Engineering, 159, Article ID: 113959. https://doi.org/10.1016/j.applthermaleng.2019.113959

[25] Said, Z., Saidur, R., Rahim, N.A. (2016). Energy and exergy analysis of a flat plate solar collector using different sizes of aluminium oxide based nanofluid. Journal of Cleaner Production, 133: 518-530. https://doi.org/10.1016/j.jclepro.2016.05.178

[26] Faizal, M., Saidur, R., Mekhilef, S., Alim, M.A. (2013). Energy, economic and environmental analysis of metal oxides nanofluid for flat-plate solar collector. Energy Conversion and Management, 76: 162-168. https://doi.org/10.1016/j.enconman.2013.07.038

[27] Nejad, M.B., Mohammed, H.A., Sadeghi, O., Zubeer, S.A. (2017). Influence of nanofluids on the efficiency of Flat-Plate Solar Collectors (FPSC). In International Conference on Advances in Energy Systems and Environmental Engineering (ASEE17), 22, p. 00123. Wroclaw, Poland: EDP Sciences.

[28] Said, Z., Sajid, M.H., Alim, M.A., Saidur, R., Rahim, N.A. (2013). Experimental investigation of the thermophysical properties of AL_2O_3-nanofluid and its effect on a flat plate solar collector. International Communications in Heat and Mass Transfer, 48: 99-107. https://doi.org/10.1016/j.icheatmasstransfer.2013.09.005

[29] Holman, V. (2011). Introduction. Visual Resources, 15(3): ix–x. https://doi.org/10.1080/01973762.1999.9658510

[30] Incropera, F.P., DeWitt, D.P. (1998). Fundamentals of Heat and Mass Transfer. Wiley.

[31] Duffie, J.A., Beckman, W.A. (1980). Solar engineering of thermal processes. New York: Wiley.

[32] Angayarkanni, S.A., Philip, J. (2015). Review on thermal properties of nanofluids: Recent developments.

Advances in Colloid and Interface Science, 225: 146-176. https://doi.org/10.1016/j.cis.2015.08.014
[33] Yu, W., Choi, S.U.S. (2003). The role of interfacial layers in the enhanced thermal conductivity of nanofluids: A renovated Maxwell model. Journal of Nanoparticle Research, 5: 167-171. https://doi.org/10.1023/A:1024438603801
[34] Buonomo, B., Cascetta, F., Cirillo, L., & Nardini, S. (2018). Application of nanofluids in solar cooling system: Dynamic simulation by means of Trnsys Software. Modell, Measurement Control B, 87(3): 143-150. http://dx.doi.org/10.18280/mmc_b.870305
[35] Xuan, Y., Roetzel, W. (2000). Conceptions for heat transfer correlation of nanofluids. International Journal of Heat and Mass transfer, 43(19): 3701-3707. https://doi.org/10.1016/S0017-9310(99)00369-5
[36] Sarkar, J. (2011). A critical review on convective heat transfer correlations of nanofluids. Renewable and Sustainable Energy Reviews, 15(6): 3271-3277. https://doi.org/10.1016/j.rser.2011.04.025
[37] Arthur, O., Karim, M.A. (2016). An investigation into the thermophysical and rheological properties of nanofluids for solar thermal applications. Renewable and Sustainable Energy Reviews, 55: 739-755. https://doi.org/10.1016/j.rser.2015.10.065
[38] Mukherjee, S., Chakrabarty, S., Mishra, P.C., Chaudhuri, P. (2020). Transient heat transfer characteristics and process intensification with Al_2O_3-water and TiO_2-water nanofluids: An experimental investigation. Chemical Engineering and Processing-Process Intensification, 150, Article ID: 107887. https://doi.org/10.1016/j.cep.2020.107887
[39] Moravej, M., Bozorg, M.V., Guan, Y., Li, L.K., Doranehgard, M.H., Hong, K., Xiong, Q. (2020). Enhancing the efficiency of a symmetric flat-plate solar collector via the use of rutile TiO_2-water nanofluids. Sustainable Energy Technologies and Assessments, 40, Article ID: 100783. https://doi.org/10.1016/j.seta.2020.100783
[40] Kurdistan Regional Government, Ministry of Electricity. (2012). https://gov.krd/moel-en/.

NOMENCLATURE

Symbols

A	Surface area (m^2)
$\mathbf{C_p}$	Heat capacity (J/kg k)
$\mathbf{F_R}$	Collector heat removal factor
$\mathbf{F_R(\tau\alpha)}$	Absorbed energy
$\mathbf{F_R(U_L)}$	Removed energy ($W/m^2.°C$)
$\mathbf{G_T}$	Solar irradiance (W/m^2)
$\mathbf{h_i}$	Inside surface convective ($W/m^2.°C$)
$\mathbf{h_o}$	Outside surface convective ($W/m^2.°C$)
$\mathbf{k}_m$	Thermal conductivity ($W/m·°C$)
$\dot{\mathbf{m}}$	Mass flow rate (kg/s)
Q_{loss}	Overall heat losses (W)
$\mathbf{Q_u}$	Supplied heat transfer (W)
R^2	Root mean square error
$\mathbf{R_{total}}$	Total thermal resistance (°C/W)
T	Temperature (°C)
U	Energy loss coefficient ($W/m^2.°C$)
$\mathbf{U_L}$	Overall heat transfer coefficient ($W/m^2.°C$)

Greek symbols

$\boldsymbol{\varphi}$	Particle concentration by weight
$\boldsymbol{\eta_{th}}$	Collector Efficiency (%)
μ	Viscosity (mPa.s)
ρ	Density (kg/m^3)
τα	Absorptance–transmittance

Subscripts

a	Ambient
bf	Base fluid
C	Collector
G	Greenhouse
H	Heat exchanger
i	Inlet
np	Nanoparticle
o	Outlet
r	Room

Abbreviations

ASHRAE	American Society of Heating, Refrigerating, and Air-conditioning Engineers
DW	Distilled Water
FPSC	Flat Plate Solar Collector
HTF	Heat Transfer Fluid
SEM	Scanning Electron Microscopes
SWHS	Solar Water Heating Systems
TRNSYS	Transient Systems Simulation